

Tm-Doped Fiber Lasers: Fundamentals and Power Scaling

Peter F. Moulton, *Senior Member, IEEE*, Glen A. Rines, *Member, IEEE*, Evgueni V. Slobodtchikov, Kevin F. Wall, Gavin Frith, Bryce Samson, and Adrian L. G. Carter

(Invited Paper)

Abstract—We describe fundamental measurements of the properties of thulium (Tm)-doped silica and power scaling studies of fiber lasers based on the material. Data on the high-lying Tm:silica energy levels, the first taken to our knowledge, indicate that pumping at 790 nm is unlikely to lead to fiber darkening via multiphoton excitation. Measurement of the cross-relaxation dynamics produces an estimate that, at the doping levels used, as much as 80% of the decay of the Tm level pumped is due to cross relaxation. Using a fiber having a 25- μm -diameter, 0.08 numerical aperture (NA) core, we observed fiber laser efficiencies as high as 64.5% and output powers of 300 W (around 2040 nm) for 500 W of launched pump power, with a nearly diffraction-limited beam. At these efficiencies, the cross-relaxation process was producing 1.8 laser photons per pump photon. We generated 885 W from a multimode laser using a 35- μm , 0.2-NA core fiber and set a new record for Tm-doped fiber laser continuous-wave power.

Index Terms—Fiber lasers, spectroscopy, thulium (Tm) doping.

I. INTRODUCTION

RECENT advances in fiber lasers have produced demonstrations of single-, double-clad fiber lasers that can generate powers exceeding 1 kW; one commercial supplier, IPG Photonics (Oxford, MA) offers a single-mode commercial product at the multikilowatt level.

To date, the highest power devices have been based on ytterbium (Yb^{3+})-doped silica fibers that operate in the wavelength region centered around 1080 nm. Lasers in this wavelength range are a serious eye hazard since they cannot be seen but their power can be imaged onto the retina. This can be a problem for some laser applications.

At present, there are two common fiber lasers that operate in the eyesafe wavelength region (>1400 nm), where optical absorption by water in the eye prevents power from reaching the retina. One laser is the ytterbium–erbium (Yb^{3+} , Er^{3+}) system at around 1550 nm, the other is the thulium (Tm^{3+}) system, tunable in the range 1850–2100 nm. The Yb, Er system can be pumped at either 940 or 980 nm, exciting the Yb

ions, which then transfer power over to the Er laser-active ions. From the pump/laser wavelength ratio, the system is limited to a maximum optical efficiency of 65%, though, in practice, the efficiency tends to fall in the 30%–40% range. In principle, if one could pump Er directly, at 1480 nm, we could obtain a much higher optical–optical efficiency, but there are practical issues in obtaining enough Er doping to get high absorption for the pump in the fiber, and diode lasers at that wavelength have yet to approach the electrical–optical efficiencies of the shorter-wavelength devices.

Tm-doped fibers are more promising at present, because it is possible to pump the Tm ions at around 790 nm, where efficient diodes are readily available, and through a cross-relaxation process, obtain two excited Tm ions for one pump photon. Thus, instead of a maximum efficiency of 41%, one can, in theory, obtain an efficiency of 82%. Starting in 1998, the power output and efficiency of double-clad, Tm-doped fibers have both steadily risen, especially with the realization that the Tm doping level could be increased with the addition of Al codoping of the core [1]–[4]. At the start of the effort to be described next, one research group had obtained a slope efficiency of 56% with respect to pump power launched into a Tm-doped silica (Tm:silica) fiber and generated 85 W of continuous-wave (CW) power [5]. In this paper, we describe our studies and experiments on some basic spectroscopy of Tm-doped silica (Tm:silica), as well as efforts to scale up the power of the Tm:silica fiber lasers.

II. SPECTROSCOPY

In working with our supplier of fibers (Nufern, Inc., East Granby, CT), we were able to obtain sections of the some of the preforms used in fiber fabrication. This provided us access to bulk-size regions of Tm:silica and allowed us to make spectroscopic measurements on the material, such as absorption and emission characterization, which might be distorted or otherwise compromised by the properties of fibers. Our work included absorption spectroscopy and characterization of the temporal decay of the energy levels involved in laser operation and pumping. It should be noted that the core sections of the preforms were codoped with several percent aluminum (Al^{3+}) to allow incorporation of the high levels of Tm needed to make cross-relaxation pumping efficient.

We studied two 3-mm thick samples [(LO) and HI] and measured absorption in the 790-nm region, using a Perkin–Elmer Lambda 9 spectrophotometer, to determine, based on available

Manuscript received October 8, 2008; revised October 29, 2008; accepted October 30, 2008. Current version published February 4, 2009. This work was supported by the High-Energy Laser Joint Technology Office.

P. F. Moulton, G. A. Rines, E. V. Slobodtchikov, and K. F. Wall are with Q-Peak, Inc., Bedford, MA 01730 USA (e-mail: moulton@qpeak.com; grines@qpeak.com; slobodtchikov@qpeak.com; kwall@qpeak.com).

G. Frith, B. Samson, and A. L. G. Carter are with Nufern, Inc., East Granby, CT 06026 USA (e-mail: gfrith@nufern.com; bsamson@nufern.com; acarter@nufern.com).

Color versions of one or more of the figures in this paper are available online at <http://ieeexplore.ieee.org>.

Digital Object Identifier 10.1109/JSTQE.2008.2010719

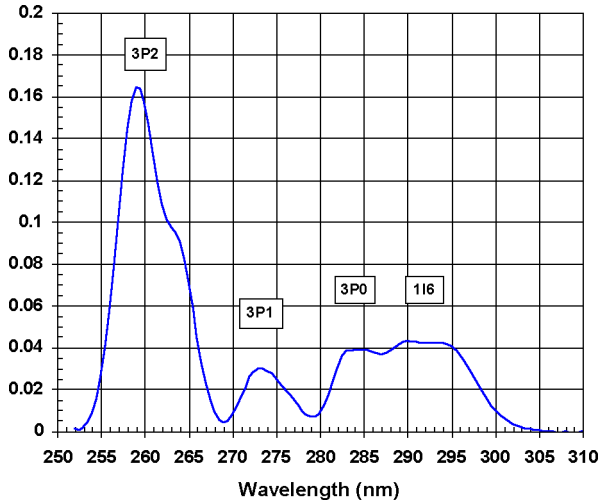


Fig. 1. Absorbance spectrum of Tm:silica sample in the UV region.

cross-section data [6], [7], the Tm doping level. The references cited show, respectively, peak cross sections for the ${}^3\text{H}_6 \rightarrow {}^3\text{H}_4$ transition of 0.85 and $1.0 \times 10^{-21} \text{ cm}^2$. Our absorption data showed the LO and HI samples thus had doping levels of 2.0 or 2.4 and 2.5 or 2.9 wt% Tm_2O_3 , depending on the reference.

In early studies of Tm:silica fibers, operated with core pumping at 1064 nm [8], the authors observed a rapid formation of optically absorbing color centers (photodarkening). The process was explained as the result of a sequential four- or five-step process through the Tm energy levels, leading to the generation of a free electron, subsequently trapped to form the color center. In order to better understand the possibility of this process occurring with 790-nm pumping, we measured visible-UV light absorption in the samples up to the short-wavelength absorption edge of the glass host to determine positions of high-lying Tm energy levels.

Even with the preform samples, the doped core regions were small in diameter, leading, with the spectrophotometer used, to baseline inaccuracies in a number of wavelength regions. We were able to get reasonably good data on the peaks of the absorption bands, through baseline corrections, up to the UV absorption edge of the core in the region of 220 nm. The pure fused silica cladding region of the preform transmitted well to the 195-nm wavelength limit of the spectrophotometer. The lower energy UV edge for the core is likely the result of the inhomogeneous nature of the doped glass. Fig. 1 shows data for the HI sample near the UV edge with the baseline corrected, and we have identified the peaks with individual Tm energy levels, which, in the glass, are Stark split but unresolved. We did not observe any higher-lying peaks.

Table I lists the peak positions of the absorption bands we observed. They are in good agreement with the energy level calculations of Gruber *et al.* for the $\text{Y}_3\text{Al}_5\text{O}_{12}$ crystal host, where we compared our peaks with the centroid of their Stark-split energy levels [9]. The calculations show that there is no higher energy level with the transparency range of the host, in agreement with our observations.

TABLE I
PEAK POSITIONS OF ABSORPTION BANDS IN Tm:SILICA

Level	Wavelength (nm)	Energy (cm^{-1})
${}^3\text{F}_4$	1670	5988
${}^3\text{H}_5$	1210	8264
${}^3\text{H}_4$	789	12674
${}^3\text{F}_3$	683	14641
${}^3\text{F}_2$	661	15129
${}^1\text{G}_4$	470	21277
${}^1\text{D}_2$	355	28209
${}^1\text{I}_6$	290	34483
${}^3\text{P}_0$	285	35149
${}^3\text{P}_1$	274	36563
${}^3\text{P}_2$	260	38536

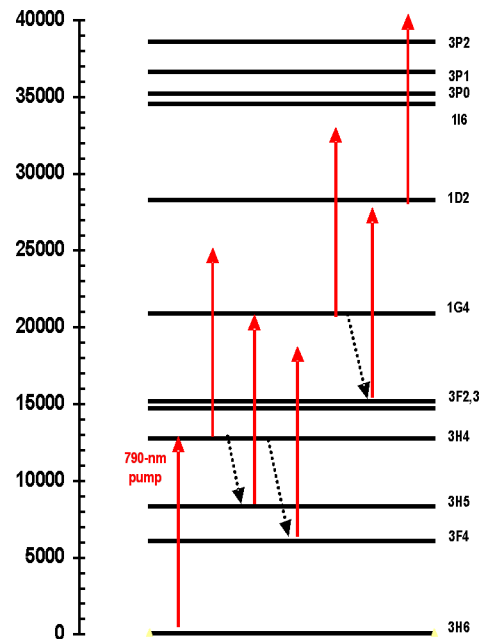


Fig. 2. Peak positions of absorption bands measured in Tm:silica with possible pumping paths associated with 790-nm photons.

In Fig. 2, we show peak energy positions of the absorption bands along with possible pumping schemes with a pump photon at 790 nm. We note the following.

- 1) There is no real transition possible from the ${}^3\text{H}_4$ level directly pumped by 790 nm to a higher lying Tm level.
- 2) Tm ions in the ${}^3\text{H}_5$ level can be pumped to the ${}^1\text{G}_4$ level responsible for the blue fluorescence observed in operating Tm fiber lasers. However, the lifetime of the ${}^3\text{H}_5$ level is very short due to nonradiative decay to the ${}^3\text{F}_4$ level. Also, the level is fed only by direct decay from the ${}^3\text{H}_4$ level, and this process is suppressed by cross-relaxation decay of the ${}^3\text{H}_4$ level into the upper laser level.

- 3) There is no real transition possible from the 3F_4 upper laser level to a higher lying Tm level.
- 4) If a Tm ion does get pumped to the 1G_4 level, there is no real transition to a higher level.
- 5) An ion in the $^3F_{2,3}$ states, populated by decay from the 1G_4 level, can make a nearly resonant transition to 1D_2 state. Because of strong nonradiative decay of the $^3F_{2,3}$ levels to the 3H_4 level, one would not expect a large population to build up in these states. In addition, the 1G_4 level can decay by a variety of processes other than into the $^3F_{2,3}$ levels.
- 6) An ion in the 1D_2 level cannot make a direct transition to a higher lying Tm level, and the energy is below that associated with strong transitions into the host electronic states, based on our UV absorption measurements.

Based on the considerations given earlier, it is evident that while there are some possible paths up the Tm energy levels to the electronic levels of the host, the paths are not straightforward, and involve lower lying levels that would not be expected to have significant populations in an operating, highly doped Tm:silica fiber laser pumped at 790 nm. For all of the transitions not resonant with actual levels, there is the possibility of virtual transitions, or those involving simultaneous emission or absorption of phonons, but these have a greatly reduced probability. There are also more complicated paths, such as upconversion involving two ions, but these require high populations in states where this is not expected. Thus, we would expect that color center formation with a 790-nm pump laser would be unlikely.

It is important to know the lifetimes of the states above the Tm ground level in Tm:silica to better understand and model the pumping and lasing properties of the Tm: fiber laser. There is some literature data on lifetimes, but discrepancies are apparent, and we expect many of the lifetimes to depend on the Tm doping level and possibly the presence of the codopant Al^{3+} ions. For measurement of the lifetime of the Tm upper laser level (3F_4), we used 10-ns-duration pulses from a gain-switched, pulse-pumped Ti:sapphire laser tuned to the 790-nm absorption band that also allowed us to obtain an estimate of the dynamics of the cross-relaxation pumping process for the upper laser level. For the $^3F_4 \rightarrow ^3H_6$ fluorescence peaking around 1800 nm, we employed a liquid-nitrogen-cooled InSb detector (Judson J10D-M204-1X4M-60) with a matched Perry 730HF preamp, with a response time faster than 1 μs . We placed an Instruments SA H-20, 20-cm grating spectrometer in front of the detector, set for a center wavelength of 1840 nm, with a bandpass of approximately 16 nm, in order to ensure that we did not sense any 2300-nm fluorescence from the $^3H_4 \rightarrow ^3H_5$ transition. We accumulated decay data in a Data Precision 6000 waveform analyzer. Fig. 3 plots data from the LO sample along with a two-component fit consisting of two exponential decays. The two components are shown as well. Decay data out to the noise limit of 0.5% of the peak signal height showed that the long component remained a good fit.

Table II summarizes our 1840-nm decay data for the LO and HI samples, showing the $1/e$ decay time, the decay time for the fast (τ_1) and slow (τ_2) components, and the ratios of the peak values and area of the fast to the slow components. In prior pub-

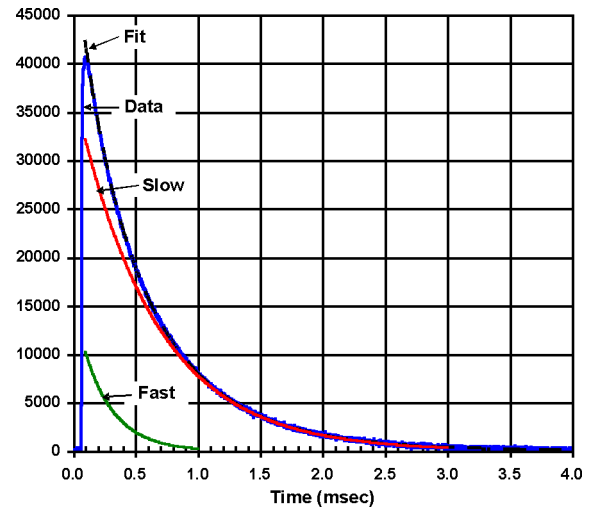


Fig. 3. Decay data for $^3F_4 \rightarrow ^3H_6$ transition fluorescence at 1840 nm along with two-component exponential fit.

TABLE II
SUMMARY OF DECAY DATA AT 1840 nm

Sample	$1/e$ (μs)	τ_1 (μs)	τ_2 (μs)	Peak ratio	Area ratio
LO	540	242	635	0.318	0.121
HI	541	273	681	0.402	0.161

lished work, a two-component decay for the $^3F_4 \rightarrow ^3H_6$ was noted as well, with slow and fast values of 111 and 650 μs [10] and 11 and 650 μs [10] for doping levels in the 1%–1.5% range. The reason for the difference between our results and prior data is unclear and suggests further investigation of Tm:silica samples with variety doping and codoping levels. With the two-component decay observed, we are dealing clearly with an inhomogeneous system. The radiative lifetime for the transition is calculated by Judd–Ofelt theory, to be in the 4.5–6 ms range [7], [11], so the lifetimes we measure are all highly non-radiative, and the inhomogeneous nature of the decay could represent the presence of two distinctly different environments for Tm ions.

In order to gain a better understanding of the cross-relaxation process, we put together apparatus to measure 800-nm region fluorescence direct from the 3H_4 level to the 3H_6 ground state. We imaged the preform fluorescence onto the entrance slit of a Spex 1681C grating spectrometer (34-cm focal length, 1200 g/mm grating) and detected the signal with a Hamamatsu R636-10 photomultiplier tube, the output of which, after amplification, went into our Data Precision 6000 waveform analyzer. Decay data from the “LO” and “HI” samples are presented in Fig. 4 and shows a highly nonexponential decay in the initial portion of the signal, with $1/e$ times indicated. When we analyzed decay at long times, we found an evolution to a single-exponent decay with decay times of 24.3 and 21.0 μs for the LO and HI samples, respectively.

The highly nonexponential initial decay is expected from the nature of the cross-relaxation process, given the distribution of spacing between pairs of Tm ions. The exponential decay in

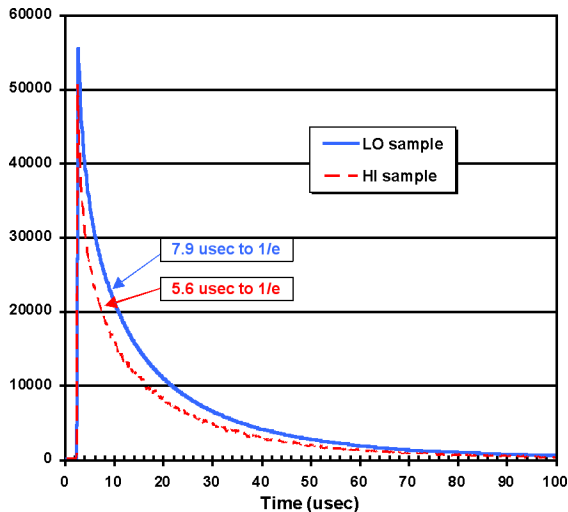


Fig. 4. Decay data for ${}^3\text{H}_4 \rightarrow {}^3\text{H}_6$ transition fluorescence at 800 nm for LO and HI samples with $1/e$ decay times indicated.

the latter portion of the signal could be explained as the signal from a single ion, not involving the cross-relaxation process. We did not have a sample with low Tm doping that we could use to measure the 800-nm decay where cross-relaxation is a minor effect. Published data [12] for a Tm:silica sample with 0.2 wt% doping indicated a measured lifetime of $45 \mu\text{s}$. Based on Judd–Ofelt analysis, the radiative lifetime for the ${}^3\text{H}_4$ level is calculated [7], [12] to fall in the $650\text{--}770 \mu\text{s}$ range, and thus, decay is clearly dominated by nonradiative processes.

If we assume that the data in [12] are substantially free from cross relaxation, then our data showing exponential decay at long times, considerably shorter than a $45\text{-}\mu\text{s}$ lifetime that represents the decay only by a single ion, require some explanation. The decay is likely not simply from isolated Tm ions. Jackson [3] has noted that rapid energy migration for ions in the ${}^3\text{H}_4$ level will take place at high Tm doping levels. Thus, the decay process can first involve migration among isolated Tm ions, then a cross relaxation that occurs when the energy reaches a site in the host material where two Tm ions are close to each other. Competing with this process is decay by a single ion that can occur with migration as well. Because of the averaging effect of migration, the migration-assisted decay process is characterized by a single rate, and thus, decay at long times appears exponential. We would expect the net decay rate to increase as the Tm concentration increases, given that the density of close ion pairs increases with concentration. Thus, our observation of a single-exponential decay process from the ${}^3\text{H}_4$ level at long times may indicate that migration of energy is an important effect in the Tm:silica.

On the basis that $45 \mu\text{s}$ is the decay time for the ${}^3\text{H}_4$ level in Tm:silica at low concentrations, and the faster decay we observe is entirely due to cross relaxation, we can determine the fraction of excitation that decays via the cross-relaxation effect, and thus determine the pumping efficiency. Changing over to decay rates rather than decay times, we assume that for a given Tm ion

$$R_T = R_S + R_{CR}$$

where R_T is the total decay rate for the ${}^3\text{H}_4$ level, R_S is the decay rate for a Tm ion in isolation, i.e., at low concentrations, and R_{CR} is the rate due to cross-relaxation. The fraction of excitation that decays by the cross-relaxation process, F_{CR} , is then

$$F_{CR} = \frac{R_{CR}}{R_T}.$$

As we note from the measured nonexponential decay, there is, in fact, a distribution of values for R_T and when we measure a decay curve it is the sum of decay from many Tm ions. We claim that, as with a single decay rate, if we integrate the observed decay curve over time for an impulse excitation, the effective, or average decay rate is inversely proportional to that integral. If we normalize the peak value of the observed decay curve to unity, do the integral, and integrate a normalized decay curve for a $45\text{-}\mu\text{s}$ lifetime, we can determine the effective, or average F_{CR} that gives us a measure of the importance of cross relaxation in the pumping process.

By integrating the normalized decay curves for the LO and HI samples and taking the ratio to the integral of normalized decay with a $45\text{-}\mu\text{s}$ lifetime, we determine that the values for F_{CR} are, respectively, 0.743 and 0.799. In the pumping process, then, we would assume that these fractions of pump photons would yield two excited laser states, while the remainder would yield just one. In terms of laser efficiency, if we assume a 795-nm pump wavelength and a 2050-nm laser wavelength, we would have maximum efficiencies of 67.6% and 69.8% for the LO and HI materials. In contrast to earlier fiber laser data [4] showing a near-linear increase in slope efficiency with doping at lower concentrations, it would appear from the spectroscopic data that concentrations above 2.5% would not yield such a linear relation. Next, we will compare this with our fiber laser data.

III. FIBER LASER STUDIES

Our fiber laser configuration, in general, involved the use of commercial, high-power, fiber-coupled diode laser sources, equipped with 793-nm-wavelength-region diode bars, coupled into a single, large-core fiber. We employed free-space optics to couple the output from the fiber into the cladding of our core-clad Tm:silica active fibers. Fig. 5 is a schematic of our experimental setup used with Laserline (Mülheim–Kärlich, Germany) LDM400-350 systems, which provided 350 W of power from a $400\text{-}\mu\text{m}$, 0.22-NA fiber.

We used two of the Laserline devices to pump the Tm:silica active fiber from both ends. The free-space optics coupling the output of the pump laser fibers into the active fiber provided a 1:1 image, well suited for coupling into our active fibers, which were designed with $400\text{-}\mu\text{m}$, 0.46-NA pump-cladding configuration. The large NA of the pump cladding resulted from the use of a polymer outer cladding. In the focused pump beam at one end of the fiber we placed a 2.5-cm-radius meniscus optic, antireflection coated on the convex surface for 790 nm, and coated on the concave surface for high transmission at 790 nm and high reflectivity at 2050 nm. When properly spaced from the active fiber, uncoated, cleaved end, the optic acted as a high reflector for the fiber laser cavity with the other mirror of

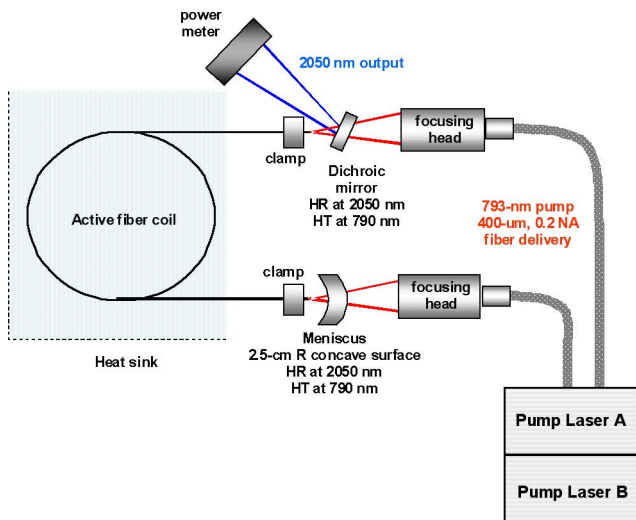


Fig. 5. Schematic of fiber laser design used with 350-W pump lasers.

the cavity being the other uncoated cleaved end of the active fiber. We extracted the fiber laser output from the uncoated end through use of a dichroic, flat mirror inserted into the pump beam.

Our characterization of the pump lasers showed that the center wavelength varied from 791 to 795 nm as the diode output power increased from low levels to full output. The spectral width [full-width at half-maximum (FWHM)] of the devices was approximately 2.5 nm. Using undoped fiber with the same pump-cladding size as our active fiber, we determined that we could launch 90% of the incident pump power into the fiber after accounting for Fresnel losses at the fiber end.

We did initial laser experiments with active fibers pulled from the LO and HI preforms, designed with nominal 20- μm -diameter, 0.2-NA cores. Using 10- and 7-m-long LO and HI fibers, respectively, we obtained about the same performance, with a slope efficiency of 46% and a maximum power of 225 W, at a nominal 2040 nm wavelength, for a launched pump power of 500 W. The launched power was our estimated value of power actually in the cladding (but not absorbed) and accounted for transport losses from the end of the pump laser fiber, through all the optics and the fiber end, and coupled into the cladding. Both fibers absorbed about 92% of the pump power.

We obtained improved performance using a fiber (LMA-HI2) with doping that was increased by about 30% over the level used for the HI preform. In addition, the fiber core size was increased to a nominal 25 μm and a “pedestal” high-index core surrounding the Tm-doped core was employed to reduce the NA to a nominal 0.08. For the laser experiments, we used an active fiber length of 5 m and had two matching core/clad, undoped fibers, 1.5-m-long, fusion-spliced to the ends of the active fiber. The use of undoped ends allowed us to more conveniently cool all of the active fiber. For cooling, we wrapped the active fiber around a 25-cm-diameter aluminum cylinder, which, in turn, was cooled by room temperature water flowing through copper tubing embedded in the cylinder.

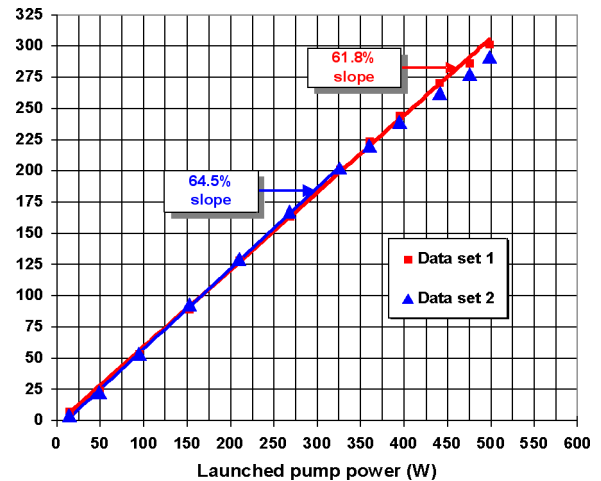


Fig. 6. Fiber laser output power versus launched pump power for LMA-HI2 fiber, showing two datasets.

Fig. 6 plots the results of input–output measurements with two datasets. In one (dataset 1), we optimized the system for the highest power, while in the other (dataset 2) we optimized for high efficiency at low powers. The cause of the rolloff at high pump powers for dataset 2 may be heating at the fiber ends and the resultant shift of the cavity alignment. The fitted slopes for datasets 1 and 2 were 61.8% and 64.5%, respectively.

We measured the wavelength of the laser to be in the region around 2040 nm. Using a fit to the beam size versus distance in the focal region formed by a long-focal-length lens, we determined that the beam M^2 was about 1.2.

Using a cutback technique with the pump laser operating at 790.5 nm, we found that transmitted pump light in the cladding of the LMA-HI2 fiber fell exponentially as the fiber length increased, with a coefficient of 0.66 m^{-1} . There was no evidence of saturation in absorbed power at long lengths, indicating that there was effective mixing of power in the cladding with that in the core. We calculated the predicted absorption of the cladding, based on the published cross sections [6], [7] and the ratio of core to cladding areas, and found agreement to the measured value within experimental error. For the 5-m length of fiber used in the laser, we calculate, given the shift of the pump wavelength center to 795 nm at high power, that about 90% of the pump light is absorbed. The best slope efficiency data, corrected for absorbed power, rises to 71.7% in good agreement with the value of 69.8% calculated by spectroscopic measurements of the HI preform dynamics, which were appropriate for Tm:silica with a 30% lower doping level. With 795-nm pumping and 2040-nm lasing, the pump quantum efficiency is 1.84.

We examined the gain spectra for Tm:silica as a function of fractional inversion, using published cross-section data for absorption and emission [7]. For the fiber laser design of Fig. 5, the minimum gain at threshold, assuming that the loss is dominated by the Fresnel reflectivity of the cleaved end, must be 31, requiring an average gain coefficient, over 5 m, of about 0.69 m^{-1} . The average fractional inversion at threshold is calculated to be 0.04–0.05. At that inversion, the gain versus wavelength relation

is nearly flat and centered around 2040 nm in good agreement with the observed laser wavelength.

The nominal V parameter for the LMA-HI2 fiber is 3.04, and thus, the fiber is not strictly single mode. Our observation of a beam M^2 of 1.2, near the diffraction limit, indicates that the fiber laser was operating primarily, if not exclusively on a single mode, perhaps as a result of increased losses for higher order modes due to the coiling of the fiber.

To scale the Tm:silica laser power higher, we employed a system similar to that shown in Fig. 5, but with two Laserline LDM1000-1000 diode sources, which provided 1 kW of power from a 1-mm-core, 0.22-NA fiber. The units supplied tuned in wavelength from 790 to 797 nm as the power increased from 200 to 1000 W with a spectral linewidth of 2 nm.

The brightness of the higher power pumps was too low for efficient coupling into the 400- μm cladding of our LMA-HI2 fiber, so we had a larger cladding fiber fabricated. The fiber, "35/625" designed with a 35- μm , 0.2-NA core and 625- μm cladding, was measured to actually have a 40- μm core (with a resultant V parameter of 12.3) and 620 μm cladding, and had the same Tm doping as the LMA-HI2 fiber. For the fiber laser experiments, we employed a 7-m length of active fiber with 1.5 m of matching core-cladding undoped fibers spliced to the ends of the active fiber.

We employed free-space optics at the end of the pump source fiber that produced a free-space beam spot with a nearly uniform power distribution having an FWHM of 520 μm . We used a length of matching undoped fiber to test the coupling of pump power into the cladding and determined that we could launch about 91% of the maximum possible pump power into the cleaved, uncoated end of the fiber.

Because of the short focal length (3 cm) of the pump-coupling optics, we had to modify the cavity design from that shown in Fig. 5. The fiber laser cavity was formed by the two uncoated, cleaved ends of the fiber assembly. We eliminated the meniscus mirror, and instead, placed a dichroic mirror in the pump beam to couple out the output power from that end of the fiber. The power output we measured was the sum of power in the beams from both ends of the fiber. We cooled the fiber by simple immersion of the active section fiber coil in a circulating, room temperature water bath. The coil diameter was approximately 40 cm.

Fig. 7 plots the data points on total power output from the 35/625 fiber laser as a function of total launched pump power, along with a linear fit to a 49.2% slope. The maximum power output, limited by the pump source, was 885 W. We measured the absorption of pump power in the fiber to be about 98%. Using a Photon, Inc. (San Jose, CA) Nanoscan laser beam profiler, with a pyroelectric detector head, we characterized the beam properties of lower power (200–350 W output) lasers based on the 35/625 fiber. We determined that the output beam had an elliptical profile (as expected from the use of coiled fiber) with M^2 -values of approximately 6 and 10 in the coil plane and orthogonal directions, respectively.

In common with the high-NA-core fiber lasers made from the LO and HI preforms, we observed a lower slope efficiency than expected given the expected efficiency of the cross-relaxation

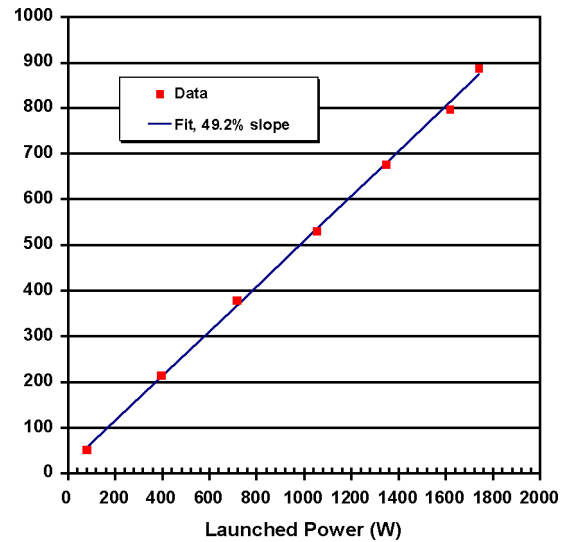


Fig. 7. Fiber laser output power versus launched pump power for 35/625 fiber, showing data and linear fit.

pumping process. The cause(s) of this is/are a current subject of investigation.

IV. CONCLUSION

One of the early concerns with Tm:silica fiber lasers was rapid degradation in output due to color center formation through a multiphoton electronic excitation process with 1064-nm-wavelength core pumping. We have investigated the spectroscopic properties of Tm:silica and concluded that the energy level structure and dynamics of the energy levels at high Tm concentrations do not support a similar process with 790-nm pumping. Due to the use of free-space optics and the resultant susceptibility of our fiber lasers to damage from contamination, we have not conducted long-term tests of the Tm:silica fiber lasers at high powers. However, in concurrent work with 790-nm-pumped Tm:silica fiber lasers at Nufern, no significant degradation in power has been observed for operational periods of several tens of hours, at the 100-W output power level [13].

We have measured the lifetime of the upper laser level of heavily doped Tm:silica and observed a two-component decay process, indicative of two distinct sets of sites for the active ions. Our dynamic measurements of the cross-relaxation pumping process indicate that with 2%–3% doping levels, one 790-nm pump photon produces, on average, about 1.8 excitations of the upper laser level, a number consistent with the best slope efficiencies we have observed in our fiber laser measurements.

Through the use of free-space-coupled, 790-nm wavelength region, cladding pumping, we have operated 2040-nm, Tm:silica fiber lasers at CW power levels of 300 W with near-diffraction-limited output, and 885 W of power in a multimode beam. We believe the latter to be the highest reported power from a Tm-doped fiber laser, and also the highest CW output from any laser operating in the 2000-nm wavelength region.

Recent work on an alternative approach to Tm:silica fiber laser pumping, using Yb, Er: fiber lasers as a resonant pumping

source, has led to CW, single-mode powers of 415 W with 720 W of 1567-nm output power [14]. The overall electrical efficiency of the laser (of the order of 12%) is limited by the efficiency of the Yb, Er: fiber laser. The system employed an all-fiber format, a design that should also be possible with advances in 790-nm pump lasers and coupling optics, with the advantage, as we and others have shown, of higher overall efficiency.

ACKNOWLEDGMENT

We gratefully acknowledge the support of K. Stebbins, A. Bark, V. Kozakevich, J. Farroni, and K. Farley in the study described earlier.

REFERENCES

- [1] S. D. Jackson and T. A. King, "High-power diode-cladding-pumped Tm-doped silica fiber laser," *Opt. Lett.*, vol. 23, pp. 1462–1464, 1998.
- [2] R. A. Hayward, W. A. Clarkson, P. W. Turner, J. Nilsson, A. B. Grudinin, and D. C. Hanna, "Efficient cladding-pumped Tm-doped silica fiber laser with high power single mode output at 2 μm ," *Electron. Lett.*, vol. 36, pp. 711–712, 2002.
- [3] S. D. Jackson and S. Mossman, "Efficiency dependence on the Tm³⁺ Al³⁺ concentrations for Tm³⁺-doped silica double-clad fiber lasers," *Appl. Opt.*, vol. 42, no. 15, pp. 2702–2707, 2003.
- [4] S. D. Jackson, "Cross relaxation and energy transfer upconversion processes relevant to the functioning of 2 μm , Tm³⁺-doped silica fiber lasers," *Opt. Commun.*, vol. 230, pp. 197–203, 2004.
- [5] G. Frith, D. G. Lancaster, and S. D. Jackson, "85W Tm³⁺-doped silica fiber laser," *Electron. Lett.*, vol. 41, no. 12, pp. 687–688, 2005.
- [6] S. D. Jackson and T. A. King, "Theoretical modeling of Tm-doped silica fiber lasers," *J. Lightw. Technol.*, vol. 17, no. 5, pp. 948–956, May 1999.
- [7] B. M. Walsh and N. P. Barnes, "Comparison of Tm:ZBLAN and Tm:silica fiber lasers; spectroscopy and tunable pulsed laser operation around 1.9 μm ," *Appl. Phys. B*, vol. 78, no. 3/4, pp. 325–333, 2004.
- [8] M. M. Broer, D. M. Krol, and D. J. DiGiovanni, "Highly nonlinear near-resonant photodarkening in a thulium-doped aluminosilicate glass fiber," *Opt. Lett.*, vol. 18, no. 10, pp. 799–801, 1993.
- [9] J. B. Gruber, M. E. Hills, R. M. Macfarlane, C. A. Morrison, G. A. Turner, G. J. Quarles, G. J. Kintz, and L. Esterowitz, "Spectra and energy levels of Tm³⁺:Y₃Al₅O₁₂," *Phys. Rev. B, Condens. Matter*, vol. 40, no. 14, pp. 9464–9478, 1989.
- [10] S. D. Jackson and T. A. King, "Efficient gain-switched operation of a Tm-doped silica fiber laser," *IEEE J. Quantum Electron.*, vol. 34, no. 5, pp. 779–789, May 1998.
- [11] S. D. Agger and J. H. Povlsen, "Emission and absorption cross section of thulium doped silica fibers," *Opt. Express*, vol. 14, no. 1, pp. 50–57, 2006.
- [12] P. Peterka, B. Faure, W. Blanc, M. Karasek, and B. Dussardier, "Theoretical modeling of S-band thulium-doped silica fiber amplifiers," *Opt. Quantum Electron.*, vol. 36, no. 1–3, pp. 201–212, 2004.
- [13] G. Frith, B. Samson, A. Carter, J. Farroni, K. Farley, and K. Tankala, "Efficient and reliable 790 nm-pumped Tm lasers from 1.91 to 2.13 μm ," *Solid State Diode Laser Technol. Rev.*, p. 200, Jun. 2008.
- [14] M. Meleshkevich, N. Platonov, D. Gapontsev, A. Drozhzhin, V. Sergeev, and V. Gapontsev, "415W Single-mode CW Thulium fiber laser in all-fiber format," in *Proc. Eur. Conf. Lasers Electro-Opt., 2007 Int. Quantum Electron. Conf. (CLEOE-IQEC 2007)*, Munich, Germany, Jun. 17–22, p. 1.



Peter F. Moulton (M'69–SM'84) received the A.B. degree in physics from Harvard College, Cambridge, MA, in 1968, and the M.S. and Ph.D. degrees from the Department of Electrical Engineering and Computer Science, Massachusetts Institute of Technology (MIT), Cambridge, in 1971 and 1975, respectively.

In 1975, he was a Postdoctoral Fellow at MIT Lincoln Laboratory, where he became a Staff Member in 1976. His research work at Lincoln Laboratory included high-resolution IR spectroscopic measurements of molecules, development of lasers for remote

sensing, and research and development of tunable and high-efficiency solid-state lasers, including invention of the Ti:sapphire laser. In 1985, he was the Vice President and General Manager of the Research Division of Schwartz Electro-Optics, where he was engaged in the research and development of a new solid-state laser materials and system. When the Research Division was spun out as a separate company, Q-Peak, Bedford, MA, he served as the Chief Technology Officer and Vice President, a position he currently holds. His current research interests include Ti:sapphire lasers, high-power diode-pumped lasers, both bulk and fiber, mid-IR solid-state lasers, nonlinear optics including parametric oscillators, medical applications of lasers, and lidar/ladar systems.

Dr. Moulton is a Fellow of the OSA and a member of the U.S. National Academy of Engineering. He was the Co-Chair of the Conference on Lasers and Electro-Optics (CLEO) and the Chairman of the CLEO Steering Committee. He was responsible for the initial organization of the Optical Society of America (OSA)/IEEE Topical Meeting on Advanced Solid-State Photonics, and has served on the Boards of the IEEE Laser and Electro-Optics Society (IEEE/LEOS) and the OSA. He was the recipient of the R.W. Wood Prize from the OSA and the William Streifer Scientific Achievement Award from the IEEE/LEOS, both in 1997.

Glen A. Rines (A'90–M'90) received the B.A. degree in physics from Gordon College, Wenham, MA, in 1977.

From 1978 to 1982, he was with Optical Fiber Technology, first at ITT Electro-Optics Products Division, Roanoke, VA, and then at Sanders Associates, Nashua, NH, where in 1982, he joined the Laser Systems Department and was engaged in the development of a variety of laser systems employing both garnet and fluoride hosts. From 1985 to 1996, he joined the Research Division of Schwartz Electro-Optics, Concord, MA where he was engaged in a wide variety of solid-state laser materials, carrying out spectroscopic analysis and laser development tasks. A significant portion of this time was dedicated to the development of Ti:Al₂O₃ laser systems. From 1996 to 2000, he was at IR Sources manufacturing laser components and custom laser systems. From 2000 to 2002, he was with the Laser Systems Group, BAE Systems, Nashua. Since 2002, he has been at Q-Peak, Bedford, MA, where he is engaged in primarily developing Ti:Al₂O₃ laser systems and fiber lasers.



Evgueni V. Slobodtchikov received the M.S. and Ph.D. degrees from Moscow State University, Moscow, Russia, in 1989 and 1993, respectively, both in laser physics.

From 1992 to 1996, he was a Researcher at Semenov Institute of Chemical Physics, Russian Academy of Sciences, Moscow, where he was engaged in the development of solid-state ultrafast and continuous-wave (CW) tunable laser systems. Between 1996 and 1999, he was a Postdoctoral Fellow, first at Osaka University, Suita, Japan, then at the University of Toronto, Toronto, ON, Canada. From 1999 to 2001, he was a Research and Development Scientist at Lambda Physik, Inc. He is currently at Q-Peak, Inc., Bedford, MA. His current research interests include ultrafast solid-state lasers and high-power fiber lasers.

Kevin F. Wall was born in Worcester, MA, on April 20, 1954. He received the B.S. degree in physics from Worcester Polytechnic Institute, Worcester, in 1976, the M.S. degree from Rensselaer Polytechnic Institute, Troy, NY, in 1980, and the Ph.D. degree in applied physics from Yale University, New Haven, CT, in 1986.

From 1979 to 1980, he was at the General Electric Research and Development Center, Schenectady, NY, where he was engaged in Mössbauer studies of amorphous magnetic materials. In 1986, he was at Massachusetts Institute of Technology (MIT) Lincoln Laboratory, where he was engaged in the development of tunable solid-state laser materials, particularly, $\text{Ti:Al}_2\text{O}_3$. From 1992 to 1997, he was at Microrac, where he was involved in the development of microchip lasers for telecommunication applications. In 1997, he joined the Research Division of Schwartz Electro-Optics (now Q-Peak), Bedford, MA, where he is currently engaged in research on diode-pumped solid-state lasers and related technologies.

Dr. Wall is a member of the Optical Society of America.

Adrian L. G. Carter received the B.Sc. degree (with first class honors) and the Ph.D. degree from the Department of Physical and Theoretical Chemistry, University of Sydney, Sydney, Australia.

In 1994, he was a Postdoctoral Research Fellow at the Technische Universität Hamburg-Harburg, Hamburg, Germany, where he was engaged in liquid crystal switching devices. In 1995, he joined the Optical Fiber Technology Center, Sydney, where he led a small group focused on the design and fabrication of novel specialty optical fibers. In 1996, he joined the Laboratory for Lightwave Technology, Brown University, as a Research Associate and was later an Assistant Professor. In 1998, he founded the specialty fiber manufacturing company Redfern Fibers, which later became Nufern, East Granby, CT, where he is currently the Chief Technology Officer (CTO).

Gavin Frith was born in Adelaide, Australia. He received the B.Eng. degree in electrical and electronic engineering from Flinders University of South Australia, Adelaide.

From 2001 to 2005, he was primarily involved in developing solid-state and fiber laser technology for electrooptic countermeasure applications with the Defence Science and Technology Organisation, Adelaide. Since 2005, he has been with Nufern, East Granby, CT, where he has been engaged in the advancement of thulium-doped silica fiber technology and devices.

Bryce Samson received the B.S. degree from Heriot-Watt University, Edinburgh, U.K., and the Ph.D. degree in semiconductor physics from the South East Essex College of Arts and Technology, Southend-on-Sea, U.K.

He was a Research Fellow at the Optoelectronics Research Center (ORC), Southampton University, Southampton, U.K., and also at the Corporate Research Laboratories, Corning, Inc. Since 2002, he has been at Nufern, where he is currently the Vice President of Business Development. His technical work has been in the spectroscopy of rare-earth-doped fibers as well as the development of Yb-, Er:Yb-, and Tm-doped fiber lasers and amplifiers. He has authored or coauthored more than 80 referred scientific, conference, and invited papers mostly in the field of optical fiber research. He is a holder of eight patents with six more patents pending.